Sigma-Point Kalman Filtering for Integrated GPS and Inertial Navigation

John L. Crassidis*

University at Buffalo, State University of New York, Amherst, NY 14260-4400

A sigma-point Kalman filter is derived for integrating GPS measurements with inertial measurements from gyros and accelerometers to determine both the position and the attitude of a moving vehicle. Sigma-point filters use a carefully selected set of sample points to more accurately map the probability distribution than the linearization of the standard extended Kalman filter, leading to faster convergence from inaccurate initial conditions in position/attitude estimation problems. The filter formulation is based on standard inertial navigation equations. The global attitude parameterization is given by a quaternion, while a generalized three-dimensional attitude representation is used to define the local attitude error. A multiplicative quaternion-error approach is used to guarantee that quaternion normalization is maintained in the filter. Simulation and experimental results are shown to compare the performance of the sigma-point filter with a standard extended Kalman filter approach.

I. Introduction

The integration of Global Positioning System (GPS) signals with Inertial Measurement Units (IMUs) has become a standard approach for position and attitude determination of a moving vehicle. An Inertial Navigation System (INS) is best described in the Preface section of the excellent book by Chatfield,[1] who states "Inertial navigation involves a blend of inertial measurements, mathematics, control system design, and geodesy." Historically, INS's were primarily used for military and commercial aircraft applications due to their high cost. However, with the advent of cheaper sensors, especially micro-mechanical ones,[2] several new applications have become mainstream, including uninhabited air vehicles, micro-robots,

*Associate Professor, Department of Mechanical & Aerospace Engineering. Email: johnc@eng.buffalo.edu.

and even guided munitions.[†] Although these cheaper sensors do not perform as well as high-grade sensors in terms of drift and white-noise measurement errors, they can be used to meet the requirements of several vehicle position/attitude knowledge specifications when aided with GPS. This allows for an attractive approach since a completely self-contained system can be used to calibrate IMUs online using GPS-determined position observations, while also determining vehicle attitude and rates in realtime.

The extended Kalman filter (EKF) is widely used in practice to blend GPS measurements with IMU data,[5,9] but it has one well-known drawback. If the errors are not within the "linear region," then filter divergence may occur. This is especially a problem for an integrated GPS/INS since, even though position is well known, attitude and IMU calibration parameters may not be well known *a prior*. In fact to this day the most researched topic for an INS has been initial alignment and attitude determination.[1] Sigma-point Kalman filters (SPKFs), such as the Unscented filter, essentially provide derivative-free higher-order approximations by approximating a Gaussian distribution rather than approximating an arbitrary nonlinear function as the EKF does.[10] They can provide more accurate results than an EKF, especially when accurate initial condition states are not well known. A sigma-point GPS/INS filter has been presented in Ref. 17, which also includes a method to fuse latency lagged observations in a theoretically consistent fashion. The attitude kinematics in that paper are based on the quaternion, which must obey a normalization constraint that can be violated in the SPKF since the predicted quaternion mean is derived using an averaged sum of quaternions. In this current paper an unconstrained three-component attitude-error vector is used to represent the quaternion error vector and the updates are performed using quaternion multiplication, leading to a natural way of maintaining the normalization constraint. This approach is an extension of the sigma-point attitude estimator, shown in Ref. 4, to the GPS/INS problem.

II. Attitude Kinematics

In this section the basic properties of attitude kinematics are summarized. The attitude matrix involves a total of nine parameters, but they are clearly not independent. Various parameterizations of the attitude matrix can be used: Euler angles, Euler axis and rotation angle, quaternions, Rodrigues parameters, etc.[16] One of the most useful attitude parameterization is given by the quaternion,[7] which is a four-dimensional vector, defined as $\mathbf{q} \equiv [\boldsymbol{\rho}^T \;\; q_4]^T$, with $\boldsymbol{\rho} \equiv [q_1 \;\; q_2 \;\; q_3]^T = \hat{\mathbf{e}} \sin(\vartheta/2)$ and $q_4 = \cos(\vartheta/2)$, where $\hat{\mathbf{e}}$ is the axis of rotation and ϑ is the angle of rotation. Since a four-dimensional vector is used to describe three dimensions, the quaternion components cannot be independent of each other. The

[†]See http://www.airpower.maxwell.af.mil/airchronicles/cc/pinker.html for recent contributions of GPS/INS to Air Force competencies.

quaternion satisfies a single constraint given by $\mathbf{q}^T\mathbf{q} = 1$, which is analogous to requiring that $\hat{\mathbf{e}}$ be a unit vector in the Euler axis/angle parameterization.[16] The attitude matrix that transforms the North-East-Down (NED) frame, N, to the body frame, B, is related to the quaternion by

$$A_N^B(\mathbf{q}) = \Xi^T(\mathbf{q})\Psi(\mathbf{q}) \tag{1}$$

with

$$\Xi(\mathbf{q}) \equiv \begin{bmatrix} q_4 I_{3\times 3} + [\boldsymbol{\rho}\times] \\ -\boldsymbol{\rho}^T \end{bmatrix}, \quad \Psi(\mathbf{q}) \equiv \begin{bmatrix} q_4 I_{3\times 3} - [\boldsymbol{\rho}\times] \\ -\boldsymbol{\rho}^T \end{bmatrix} \tag{2}$$

where $[\boldsymbol{\rho}\times]$ is the cross product matrix, defined in Ref. 11. An advantage to using quaternions is that the attitude matrix is quadratic in the parameters and also does not involve transcendental functions.

The quaternion kinematics equation is given by

$$\dot{\mathbf{q}} = \frac{1}{2}\Xi(\mathbf{q})\boldsymbol{\omega}_{B/N}^B \tag{3}$$

where $\boldsymbol{\omega}_{B/N}^B$ is angular velocity of the B frame relative to the N frame expressed in B coordinates. A major advantage of using quaternions is that the kinematics equation is linear in the quaternion and is also free of singularities. Another advantage of quaternions is that successive rotations can be accomplished using quaternion multiplication. Here we adopt the convention of Lefferts, Markley, and Shuster[11] who multiply the quaternions in the same order as the attitude matrix multiplication (in contrast to the usual convention established by Hamilton[7]). Suppose we wish to perform a successive rotation. This can be written using $A(\mathbf{q}')A(\mathbf{q}) = A(\mathbf{q}' \otimes \mathbf{q})$. The composition of the quaternions is bilinear, with $\mathbf{q}' \otimes \mathbf{q} = [\Psi(\mathbf{q}') \;\; \mathbf{q}']\,\mathbf{q} = [\Xi(\mathbf{q}) \;\; \mathbf{q}]\,\mathbf{q}'$. Also, the inverse quaternion is defined by $\mathbf{q}^{-1} \equiv [-\boldsymbol{\rho}^T \;\; q_4]^T$. Note that $\mathbf{q} \otimes \mathbf{q}^{-1} = [0 \;\; 0 \;\; 0 \;\; 1]^T$, which is the identity quaternion. A computationally efficient algorithm to extract the quaternion from the attitude matrix is given in Ref. 15.

III. Gyro and Accelerometer Models

The gyro measurement model is given by[6]

$$\tilde{\boldsymbol{\omega}}_{B/I}^B = (I_{3\times 3} + \mathcal{K}_g)\boldsymbol{\omega}_{B/I}^B + \mathbf{b}_g + \boldsymbol{\eta}_{gv} \tag{4a}$$

$$\dot{\mathbf{b}}_g = \boldsymbol{\eta}_{gu} \tag{4b}$$

where $\boldsymbol{\omega}_{B/I}^B$ is the true angular velocity of the B frame relative to the inertial frame, I, expressed in B coordinates, $\tilde{\boldsymbol{\omega}}_{B/I}^B$ is the gyro measurement, $\mathbf{b}_g$ is the gyro "bias" derived from a random walk process, $\mathcal{K}_g$ is a diagonal matrix of gyro scale factors, and $\boldsymbol{\eta}_{gv}$ and $\boldsymbol{\eta}_{gu}$

are zero-mean Gaussian white-noise processes with spectral densities given by $\sigma_{gv}^2 I_{3\times3}$ and $\sigma_{gu}^2 I_{3\times3}$, respectively. The accelerometer measurement model follows along the same lines as the gyro model.[9] Simulating gyro and accelerometer using computers is not easy since continuous measurements cannot be generated using digital computers. A discrete-time simulation is possible using the spectral densities though.[3]

IV. Sigma-Point GPS/INS Filter

A review of the GPS/INS equations can be found in Refs. 5 and 9. Also, a review of the standard sigma-point filter equations, using symbols consistent with those in this paper, can be found in Ref. 18. This filter is straightforward for GPS/INS applications, except for the quaternion normalization. Since the predicted quaternion mean is derived using an averaged sum of quaternions, no guarantees can be made that the resulting quaternion will have unit norm. This makes straightforward implementation of the SPKF with quaternions undesirable. A better way involves using an unconstrained three-component vector to represent an attitude error quaternion.[4] We begin by defining the following state vector, where the superscript + denotes an update:

$$\begin{aligned}\boldsymbol{\chi}_k(0) = \hat{\mathbf{x}}_k^+ &\equiv \begin{bmatrix}(\boldsymbol{\delta}\hat{\mathbf{s}}_k^+)^T & (\hat{\mathbf{p}}_k^+)^T & (\hat{\mathbf{v}}_k^{N+})^T & (\hat{\mathbf{b}}_{g_k}^+)^T & (\hat{\mathbf{b}}_{a_k}^+)^T & (\hat{\mathbf{k}}_{g_k}^+)^T & (\hat{\mathbf{k}}_{a_k}^+)^T\end{bmatrix}^T \\ \boldsymbol{\chi}_k(i) &\equiv \begin{bmatrix}[\boldsymbol{\chi}_k^{\delta s}(i)]^T & [\boldsymbol{\chi}_k^{p}(i)]^T & [\boldsymbol{\chi}_k^{V^N}(i)]^T & [\boldsymbol{\chi}_k^{b_g}(i)]^T & [\boldsymbol{\chi}_k^{b_a}(i)]^T & [\boldsymbol{\chi}_k^{\mathcal{K}_g}(i)]^T & [\boldsymbol{\chi}_k^{\mathcal{K}_a}(i)]^T\end{bmatrix}^T\end{aligned} \tag{5}$$

where $\boldsymbol{\delta}\hat{\mathbf{s}}_k^+$ is used to propagate and update a nominal quaternion, $\hat{\mathbf{p}}_k^+$ is the estimated position consisting of the latitude, λ, longitude, Φ, and height, h, $\hat{\mathbf{v}}_k^{N+}$ is the estimated velocity vector, $\hat{\mathbf{b}}_{g_k}^+$ and $\hat{\mathbf{b}}_{a_k}^+$ are the estimated gyro and accelerometer biases, respectively, and $\hat{\mathbf{k}}_{g_k}^+$ and $\hat{\mathbf{k}}_{a_k}^+$ are the the estimated gyro and accelerometer scale factors, respectively. The vector $\boldsymbol{\chi}_k(i)$ is derived from the "sigma points" taken from a decomposition of the error-covariance matrix (see Ref. 18 for more details). Since the three-dimensional attitude-error representation is unconstrained, the resulting overall covariance matrix is a 21×21 matrix. The first three components of the vector $\boldsymbol{\chi}_k(i)$ in Eq. (5) are defined by $\boldsymbol{\chi}_k^{\delta s}(i)$. To describe $\boldsymbol{\chi}_k^{\delta s}$ we first define a new quaternion generated by multiplying an error quaternion by the current estimate:

$$\hat{\mathbf{q}}_k^+(0) = \hat{\mathbf{q}}_k^+ \tag{6a}$$

$$\hat{\mathbf{q}}_k^+(i) = \boldsymbol{\delta}\mathbf{q}_k^+(i) \otimes \hat{\mathbf{q}}_k^+, \quad i = 1, 2, \ldots, 42 \tag{6b}$$

with $\boldsymbol{\delta}\mathbf{q}_k^+(i) \equiv \left[\boldsymbol{\delta}\boldsymbol{\rho}_k^{+T}(i) \;\; \delta q_{4_k}^+(i)\right]^T$ represented by the generalized Rodrigues parameters:[14]

$$\delta q_{4_k}^+(i) = \frac{-c\,||\boldsymbol{\chi}_k^{\delta s}(i)||^2 + f\sqrt{f^2 + (1-c^2)||\boldsymbol{\chi}_k^{\delta s}(i)||^2}}{f^2 + ||\boldsymbol{\chi}_k^{\delta s}(i)||^2}, \quad i = 1, 2 \ldots, 42 \tag{7a}$$

$$\boldsymbol{\delta}\boldsymbol{\rho}_k^+(i) = f^{-1}\left[c + \delta q_{4_k}^+(i)\right]\boldsymbol{\chi}_k^{\delta s}(i), \quad i = 1, 2, \ldots, 42 \tag{7b}$$

where c is a parameter from 0 to 1, and f is a scale factor chosen to be $f = 2(c+1)$.[4] Equation (6a) clearly requires that $\boldsymbol{\chi}_k^{\delta s}(0)$ be zero. This is due to the reset of the attitude error to zero after the previous update, which is used to move information from one part of the estimate to another part.[12] This reset rotates the reference frame for the covariance, so we might expect the covariance to be rotated, even though no new information is added. But the covariance depends on the assumed statistics of the measurements, not on the actual measurements. Therefore, since the update is zero-mean, the mean rotation caused by the reset is actually zero, so the covariance is in fact not affected by the reset. Next, the updated quaternions are propagated forward using Eq. (3) with the estimated angular velocities given by $\hat{\boldsymbol{\omega}}_{B/N}^B(i) = [I_{3\times3} - \boldsymbol{\chi}^{\mathcal{K}_g}(i)]\left[\tilde{\boldsymbol{\omega}}_{B/I}^B - \boldsymbol{\chi}^{b_g}(i)\right] - A_N^B[\hat{\mathbf{q}}(i)]\boldsymbol{\omega}_{N/I}^N$, $i = 0, 1, \ldots, 42$, where $\boldsymbol{\chi}^{\mathcal{K}_g}(i)$ and $\boldsymbol{\chi}^{b_g}(i)$ are formed from the gyro scale-factor and bias sigma points, respectively. The propagated error quaternions are computed using $\boldsymbol{\delta}\mathbf{q}_{k+1}^-(i) = \hat{\mathbf{q}}_{k+1}^-(i) \otimes \left[\hat{\mathbf{q}}_{k+1}^-(0)\right]^{-1}$, $i = 0, 1, \ldots, 42$. Note that $\boldsymbol{\delta}\mathbf{q}_{k+1}^-(0)$ is the identity quaternion. Finally, the propagated sigma points can be computed using[4]

$$\boldsymbol{\chi}_{k+1}^{\delta s}(0) = \mathbf{0} \tag{8a}$$

$$\boldsymbol{\chi}_{k+1}^{\delta s}(i) = f\frac{\boldsymbol{\delta}\boldsymbol{\rho}_{k+1}^-(i)}{c + \delta q_{4_{k+1}}^-(i)}, \quad i = 1, 2, \ldots, 42 \tag{8b}$$

with $\left[\boldsymbol{\delta}\boldsymbol{\rho}_{k+1}^{-T}(i) \;\; \delta q_{4_{k+1}}^-(i)\right]^T = \boldsymbol{\delta}\mathbf{q}_{k+1}^-(i)$. The predicted mean and covariance can now be computed using the standard SPKF equations. A flow chart for the quaternion update process is shown in Figure 1 (see Ref. 3 for an explanation of the symbols).

V. Simulation Results

In this section simulation results are shown that estimate for a moving vehicle's attitude, position and velocity, as well as the gyro and accelerometer biases and scale factors. The simulation parameters are shown in Table 1. A standard EKF with quaternions is used in the comparisons.[13] Note that all measurements (GPS pseudoranges, gyros and accelerometers) are assumed to be sampled every 1 second, which isn't true in practice. This further stresses the performance of the filters for the comparisons between the EKF and SPKF. The total

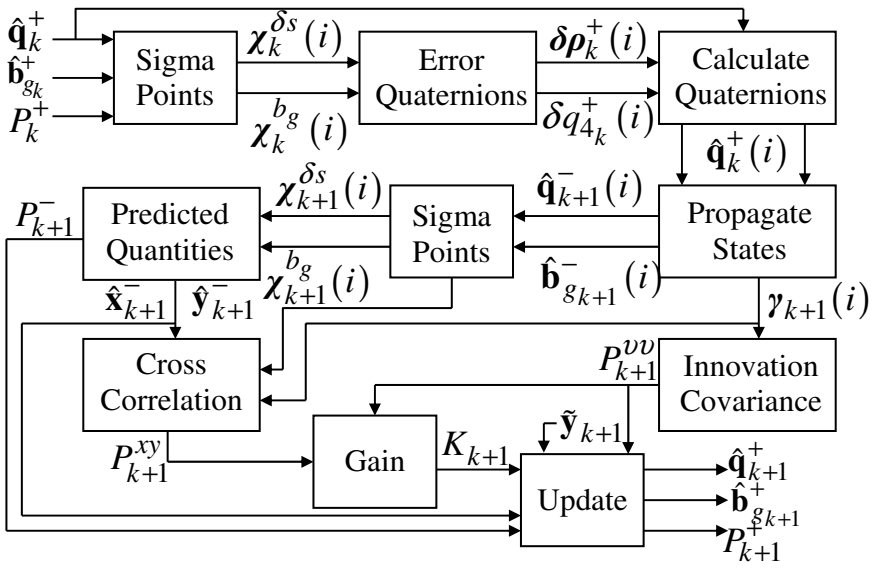

Figure 1: Flow Chart for Quaternion Update in the SPKF

time of the simulation is 8 minutes. The initial quaternion is given so that the vehicle body frame is aligned with the local NED frame. The acceleration inputs are given by: zero for the north and east accelerations, with the down acceleration set to the initial acceleration of gravity. The rotational rate profile is given by: 5 deg/min rotation about the x axis for the first 160 seconds and then zero for the final 320 seconds; no rotation about the y axis for the first 160 seconds, then a 5 deg/min rotation for the next 160 seconds and zero for the final 160 seconds; no rotation about the z axis for the first 320 seconds, then 5 deg/min rotation for the final 160 seconds. The GPS constellation is simulated using GPS week 137 and a time of applicability of 61440.0000 seconds (see Ref. 8 for an explanation of GPS time). Using the position profile the number of GPS satellites available can be computed using a 15° elevation cutoff.[8] The number of available GPS satellites over time ranges from a minimum of 5 satellites to a maximum of 6 satellites. The clock-bias drift is modelled using a random walk process: $\dot{\tau} = w_\tau$, where the variance (in seconds) of w_τ is given by 200. GPS measurements are obtained using a standard deviation of 5 meters for the white-noise errors.

Using all available GPS pseudoranges a position in cartesian components is determined using nonlinear least squares, which is then converted into longitude, latitude and height. These quantities are used as "measurements" in the filters, where the covariance is computed from the nonlinear least-squares solution. The approach corresponds to a "loose" GPS/INS configuration. When the initial conditions are "close" to the true values, both the EKF and SPKF gave identical results with good filter convergence. In general, position is very well known but attitude is not. To test the robustness of the EKF an initial attitude error of 15 degrees is given in each axis. This error is not unrealistic for an actual application. The

Table 1: Simulation Parameters

Sampling Interval	$\Delta t = 1$ sec
Gyro	$\sigma_{gv} = 2.9089 \times 10^{-7}$ rad/sec$^{1/2}$ $\sigma_{gu} = 9.1989 \times 10^{-7}$ rad/sec$^{3/2}$
Accelerometer	$\sigma_{av} = 9.8100 \times 10^{-5}$ m/sec$^{3/2}$ $\sigma_{au} = 6.0000 \times 10^{-5}$ m/sec$^{5/2}$
Initial Biases	$\mathbf{b}_g(t_0) = 10\,[1\ \ 1\ \ 1]^T$ deg/hr $\mathbf{b}_a(t_0) = 0.003\,[1\ \ 1\ \ 1]^T$ m/s^2
Scale Factors	$\mathcal{K}_g = 0.01 I_{3\times 3}$ $\mathcal{K}_a = 0.005 I_{3\times 3}$
Vehicle Origin	$\lambda(t_0) = 38°$, $\Phi(t_0) = -77°$, $h(t_0) = 0$ m
Initial Attitude	$\mathbf{q}(t_0) = [0\ \ 0\ \ 0\ \ 1]^T$
Initial Velocity	$\mathbf{v}^N(t_0) = [200\ \ 200\ \ -10]^T$ m/s

initial covariance matrix P_0 in the EKF is diagonal. For this case, the three attitude parts of the initial covariance are each set to a 3σ bound of 15 degrees, i.e. $[(15/3) \times (\pi/180)]^2$ rad^2. The initial estimates for position are set to the true latitude, longitude and height. The initial variances for latitude and longitude are each given by $(1 \times 10^{-6})^2$ rad^2. The initial variance for height is given by $(20/3)^2$ m^2. To further stress the filters the initial velocity is set to zero. For this case, the initial variances in the filters for the north and east velocities are each set to $(200/3)^2$ and the initial variance for down velocity is set to $(10/3)^2$. The initial gyro and accelerometer biases and scale factors are all set to zero. The three gyro-bias parts of the initial covariance are each set to a 3σ bound of 30 degrees per hour, i.e. $[(30/3) \times (\pi/(180 \times 3600))]^2$. The three accelerometer-bias parts of the initial covariance are each set to a 3σ bound of 0.005 meters per second-squared, i.e. $(0.005/3)^2$. The three gyro-scale factor parts of the initial covariance are each set to a 3σ bound of 0.015, i.e. $(0.015/3)^2$. Finally, the three accelerometer-scale factor parts of the initial covariance are each set to a 3σ bound of 0.010, i.e. $(0.010/3)^2$.

The resulting EKF attitude errors for a typical case are shown in Figure 2(a). The attitude errors diverge and significantly drift outside their respective 3σ bounds, which indicates that the EKF is performing in a subpar fashion. This is due to the large initial errors that are not handled well in the linearization of the dynamic model in the EKF. However, the

SPKF attitude errors are much closer to their respective 3σ bounds than the EKF attitude errors, as shown in Figure 2(b). The larger errors in yaw are due to the fact that this angle is the least observable state for the particular vehicle motion. The biggest concern with the EKF solutions is the confidence of the results dictated by the 3σ bounds. In fact, if the truth is not known *a prior* and we only had the covariance to assess filter performance, this plot would indicate that the EKF is performing better than the SPKF. This can certainly provide some misleading results when using the EKF with large initial condition errors. A comparison of the gyro bias estimates between the EKF and SPKF is shown by Figures 2(c) and 2(d), respectively. The errors for the EKF drift outside of their respected 3σ bounds for every axis. However, the SPKF bias errors are much closer to their 3σ bounds than the EKF bias errors, as shown in Figure 2(d). These simulation results indicate that the SPKF is able to provide more robust characteristics than an EKF for GPS/INS applications. Another simulation has been executed where the initial attitude and velocity are close to their respective true values, but large initial bias values, e.g. 100 deg/hr for the gyros, have been used. The performance characteristics of these results are similar to the results shown in Figure 2, with the SPKF showing better convergence properties than the EKF.

Experimental data has been obtained from the inertial navigation system for the NC-131 Total In-Flight Simulator (TIFS) aircraft. The TIFS aircraft is a highly modified Convair-580 twin turboprop transport and its primary use has been in the development and evaluation of new aircraft flying qualities, flight controls, and cockpit displays, as well as general flight research. The GPS determined position is given in 1 second intervals, while the INS provides gyro and accelerometer data at 0.01 second intervals. A 30 second data span is provided under modest aircraft motions, as shown by the onboard filter solution given in Figure 3. When the initial conditions provided from the onboard solution are used in the EKF and SPKF algorithms, both filters provide nearly identical results as the onboard solution for all states. In order to test the robustness of the EKF and SPKF algorithms, deviations of 5% in the initial roll, pitch and yaw angles are provided. The three attitude parts of the initial covariance are each set to a 3σ bound of 0.5 degrees, i.e. $[(0.5/3) \times (\pi/180)]^2$ rad^2. Results are compared with the onboard solutions for both filters. The most dramatic results are given by the attitude differences. A plot of the pitch angle differences between the onboard solution and the EKF/SPKF algorithms is shown in Figure 4. Note that only 30 updates for the GPS measurements are given, due to the short data span. Still, the results indicate that the SPKF has the ability to converge faster to the onboard computed solution, i.e. the solution with no initial attitude errors, than the EKF. Similar results are obtained for roll and yaw.

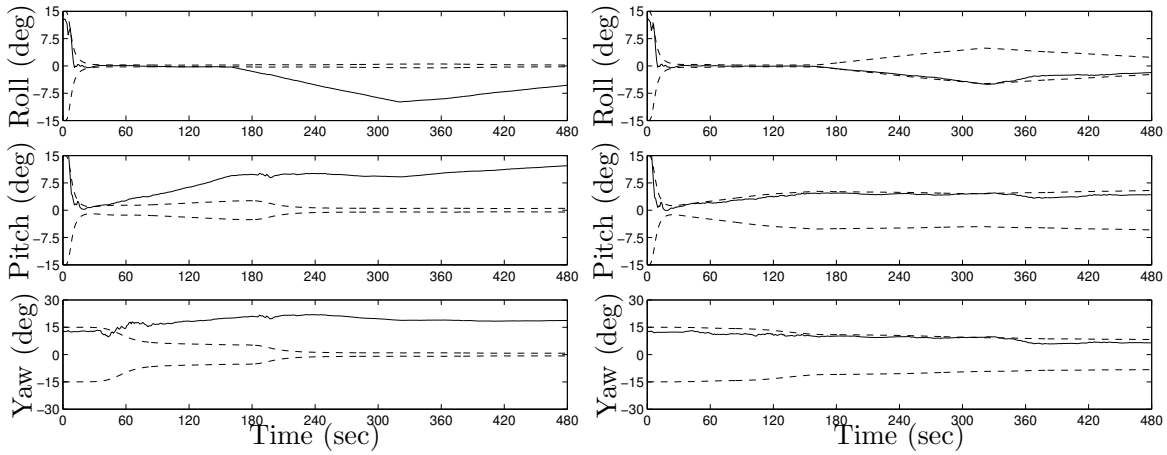

(a) EKF Attitude Errors and 3σ Bounds

(b) SPKF Attitude Errors and 3σ Bounds

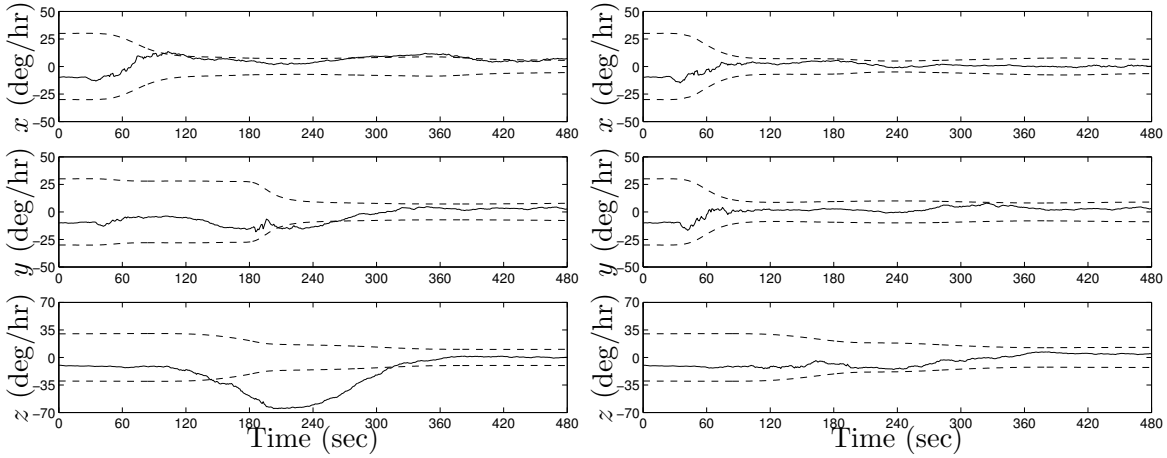

(c) EKF Gyro-Bias Errors and 3σ Bounds

(d) SPKF Gyro-Bias Errors and 3σ Bounds

Figure 2: EKF and SPKF Results for Large Initial Errors

VI. Conclusions

In this paper a sigma-point filter formulation was shown for the purpose of GPS/INS applications. The filter is based on a quaternion parameterization of the attitude. However, straightforward implementation of the sigma-point filter using quaternion kinematics did not produce a unit quaternion estimate. To overcome this difficulty the quaternion was represented by a three-dimensional vector of generalized Rodrigues parameters, which also reduced the size the covariance matrix. Simulation and experimental results indicated that the performance of the sigma-point filter exceeds the standard extended Kalman filter for large initialization errors.

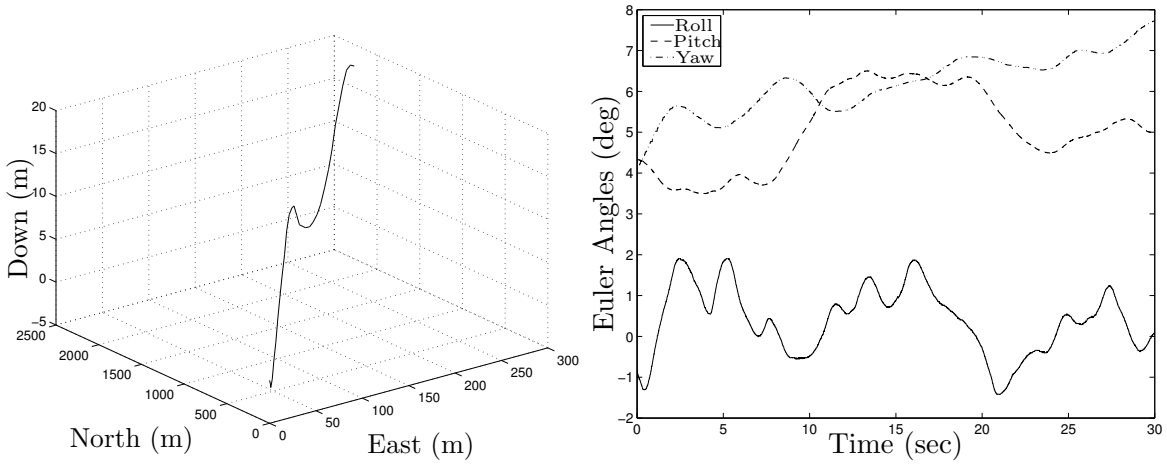

(a) Position (b) Attitude

Figure 3: NED Position and Attitude

Acknowledgements

This work was funded by the DOE NNSA NA-22 Proliferation Detection Program Office, Advanced Radar Systems project, under the guidance of Theodore Kim and Curtis Webb at Sandia National Laboratories. The author greatly appreciates this support. Data from the TIFS aircraft has been provided by the Calspan Corporation.

References

[1]A. B. Chatfield, *Fundamentals of High Accuracy Inertial Navigation*. Reston, VA: American Institute of Aeronautics and Astronautics, Inc., 1997.

[2]J. Connelly, A. Kourepenis, T. Marinis, and D. Hanson, "Micromechanical sensors in tactical GN&C applications," in *AIAA Guidance, Navigation and Contol Conference*, Montreal, QB, Canada, Aug. 2001, AIAA-2001-4407.

[3]J. L. Crassidis, "Sigma-point Kalman filtering for integrated GPS and inertial navigation," in *AIAA Guidance, Navigation and Contol Conference*, San Francisco, CA, Aug. 2005, AIAA-2005-6052.

[4]J. L. Crassidis and F. L. Markley, "Unscented filtering for spacecraft attitude estimation," *Journal of Guidance, Control, and Dynamics*, vol. 26, no. 4, pp. 536–542, July-Aug. 2003.

[5]J. Farrell and M. Barth, *The Global Positioning System & Inertial Navigation*. New York, NY: McGraw-Hill, 1998.

[6]R. L. Farrenkopf, "Analytic steady-state accuracy solutions for two common spacecraft attitude estimators," *Journal of Guidance and Control*, vol. 1, no. 4, pp. 282–284, July-Aug. 1978.

[7]W. R. Hamilton, *Elements of Quaternions*. London, England: Longmans, Green and Co., 1866.

[8]B. Hofmann-Wellenhof, H. Lichtenegger, and J. Collins, *GPS: Theory and Practice*, 5th ed. New York, NY: Springer Wien, 2001.

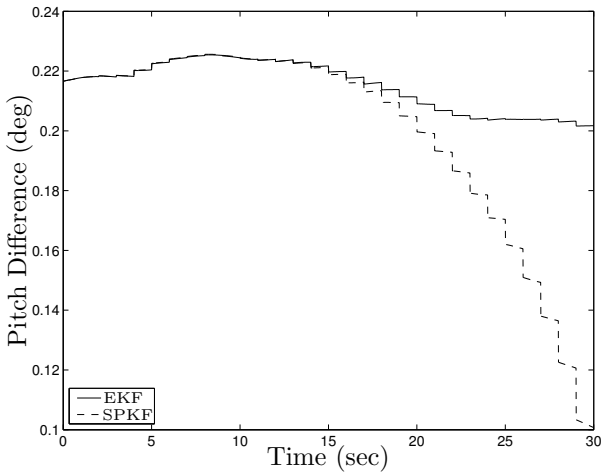

Figure 4: EKF and SPKF Estimate Differences for Pitch Angle

[9]C. Jekeli, *Inertial Navigation Systems with Geodetic Applications*. Berlin, Germany: Walter de Gruyter, 2000.

[10]S. J. Julier, J. K. Uhlmann, and H. F. Durrant-Whyte, "A new method for the nonlinear transformation of means and covariances in filters and estimators," *IEEE Transactions on Automatic Control*, vol. AC-45, no. 3, pp. 477–482, March 2000.

[11]E. J. Lefferts, F. L. Markley, and M. D. Shuster, "Kalman filtering for spacecraft attitude estimation," *Journal of Guidance, Control, and Dynamics*, vol. 5, no. 5, pp. 417–429, Sept.-Oct. 1982.

[12]F. L. Markley, "Attitude error representations for Kalman filtering," *Journal of Guidance, Control, and Dynamics*, vol. 26, no. 2, pp. 311–317, March-April 2003.

[13]R. M. Rogers, *Applied Mathematics in Integrated Navigation Systems*, 2nd ed. Reston, VA: American Institute of Aeronautics and Astronautics, Inc., 2003, ch. 15.

[14]H. Schaub and J. L. Junkins, "Stereographic orientation parameters for attitude dynamics: A generalization of the Rodrigues parameters," *Journal of the Astronautical Sciences*, vol. 44, no. 1, pp. 1–20, Jan.-March 1996.

[15]S. W. Shepperd, "Quaternion from rotation matrix," *Journal of Guidance and Control*, vol. 1, no. 3, pp. 223–224, May-June 1978.

[16]M. D. Shuster, "A survey of attitude representations," *Journal of the Astronautical Sciences*, vol. 41, no. 4, pp. 439–517, Oct.-Dec. 1993.

[17]R. van der Merwe, E. A. Wan, and S. I. Julier, "Sigma-point Kalman filters for nonlinear estimation and sensor-fusion: Applications to integrated navigation," in *AIAA Guidance, Navigation and Contol Conference*, Providence, RI, Aug. 2004, AIAA-2004-5120.

[18]E. Wan and R. van der Merwe, "The unscented Kalman filter," in *Kalman Filtering and Neural Networks*, S. Haykin, Ed. New York, NY: John Wiley & Sons, 2001, ch. 7.